Review

Multiphoton Tomography in Cosmetic Research

Karsten König * and Aisada König

Posted Date: 25 December 2024

doi: 10.20944/preprints202412.2129.v1

Keywords: skin care; cosmetics; multiphoton tomography; two-photon microscopy; antiaging; collagen; melanin; hair; antioxidants; virtual biopsy

Review

Multiphoton Tomography in Cosmetic Research

Karsten König * and Aisada König

JenLab GmbH, Johann-Hittorf-Strasse 8, 12559 Berlin, Germany

* Correspondence: info@jenlab.de

Abstract: Background: Multiphoton tomography (MPT) is a femtosecond laser imaging technique that enables high-resolution virtual biopsies of human skin. It provides a non-invasive method for analyzing cellular metabolism, structural changes, and responses to cosmetic products, providing insights into cell-cosmetic interactions. This review explores the principles, historical development, and key applications of MPT in cosmetic research. Methods: The latest MPT device combines five modalities: (i) two-photon fluorescence: visualizes cells, elastin, and cosmetic ingredients; (ii) second harmonic generation (SHG): maps the collagen network; (iii) fluorescence lifetime imaging (FLIM): differentiate eumelanin from pheomelanin and evaluates the impact of cosmetics on cellular metabolic activity (iv) reflectance confocal microscopy (RCM): images cell membranes and cosmetic particles, and (v) white LED imaging for dermoscopy. Results: MPT enables in-depth examination of extracellular matrix changes, cellular metabolism, and melanin production. It identifies skin responses to cosmetic products and tracks the intratissue distribution of sunscreen nanoparticles, nano- and microplastics, and other cosmetic components. Quantitative measurements, such as the elastin-to-collagen ratio, provide insights into anti-aging effects. Conclusions: MPT is a powerful *in vivo* imaging tool for the cosmetic industry. Its superior resolution and metabolic information facilitate the evaluation of product efficacy and support the development of personalized skincare solutions.

Keywords: skin care; cosmetics; multiphoton tomography; two-photon microscopy; antiaging; collagen; melanin; hair; antioxidants; virtual biopsy

1. Introduction

There is an increasing need in the cosmetic industry for high-resolution, non-invasive optical imaging methods of human skin to avoid physical biopsies, animal testing and to study the cosmetic product efficacy in the natural physiological environment of *in vivo* human skin.

The intratissue accumulation of cosmetic ingredients and their effects on the skin state over time are of particular interest. The development of non-invasive optical 3D skin imaging methods replaces physical skin biopsies in cosmetic clinical research and permits long-term skin studies, such as skin-cosmetic product interactions. Optical imaging enables the creation of personalized skin care solutions. Particularly noteworthy is imaging of the epidermis and the papillary dermis with submicron resolution to analyze both structural changes and metabolic state of living epidermal cells. Furthermore, researchers seek to gather information on the collagen-elastin network.

Optical coherence tomography (OCT) [1–3], photoacoustic tomography (PAT) [4], and reflectance confocal microscopy (RCM) [5] are used techniques for 3D skin imaging.

However, multiphoton tomography (MPT) surpasses these methods in spatial resolution and functional capabilities [6]. MPT devices, equipped with a numerical aperture of 1.3, achieve a lateral resolution of up to 300 nanometers, enabling the imaging of single mitochondria, the dendrites of melanocytes, and elastin fibers without external labeling. Additionally, MPT allows visualization of the collagen network through a process known as second harmonic generation (SHG). The cell's

 doi:10.20944/preprints202412.2129.v1

metabolism can be investigated by imaging fluorescent coenzymes such as nicotinamide adenine dinucleotide (NADH) and flavin adenine dinucleotide (FAD).

This review provides (i) an overview of the principle of MPT, (ii) the three generations of multiphoton tomographs, (iii) a historical overview of MPT studies on human volunteers in cosmetic research (iv) key application fields of MPT in cosmetic research, and (v) the role of artificial intelligence (AI) in enhancing MPT image acquisition and processing.

2. Principle of Multiphoton Tomography

MPT is a nonlinear imaging technique based on femtosecond laser scanning microscopy, which enables optical sectioning through localized two-photon absorption within the focal volume of high numerical aperture focusing optics. The phenomenon of two-photon absorption was first predicted by *Maria Goeppert (*Nobel prize winner*)* in 1931 during her PhD research [7] and later realized experimentally by *Wolfgang Kaiser* and *Charles Garrett* in 1961, shortly after the invention of the laser [8].

In 1990, Winfried Denk, Strickler, and Watt W Webb built the first two-photon fluorescence microscope, revolutionizing optical imaging [9]. A decade later, Karsten König realized the first multiphoton tomograph for label-free, *in vivo* imaging of human skin based on a near infrared (NIR) femtosecond titanium:sapphire laser [6]. Turn-key, robust, and tunable Ti:sapphire lasers are the preferred light source for multiphoton imaging due to their broad spectral range (from 700 nm to about 1000 nm), which spans the dark red and the NIR regions. Recently, ultracompact erbium-doped femtosecond fiber lasers operating at 780 nm have been employed for multimodal multiphoton tomography of *in vivo* human skin for cosmetic research and the detection of black skin cancer (malignant melanoma) [10].

Figure 1 illustrates the principle of two-photon excitation. Two NIR photons are absorbed simultaneously to provide the energy required for fluorescence emission in the visible spectrum. For instance, two NIR photons at 780 nm provide the same energy as a single UV photon at 390 nm. Therefore, the near infrared laser with its superior light penetration depth can excite intratissue fluorophores, such as reduced coenzyme NADH, that typically require UV light. UV does not penetrate deep and may induce phototoxic effects.

In addition to two-photon excited fluorescence, the process of second harmonic generation (SHG) occurs if the femtosecond laser beam interacts with non-centrosymmetric skin structures in the skin, such as collagen fibers. In that case, an SHG signal at exactly half the laser wavelength is generated. For example, collagen provides UV photons at 390 nm when exposed to a 780 nm laser beam.

MPT offers superior imaging compared to UV and visible light-based techniques, as NIR radiation penetrates deeper into the skin. However, the imaging depth is constrained by the working distance of the focusing optics, which is approximately 0.2 mm.

MPT of skin combines two-photon excited autofluorescence (AF) imaging and SHG imaging. There are a variety of endogenous skin fluorophores, such as coenzymes, keratin, melanin, porphyrins, and elastin [11,12].

The mean fluorescence lifetime of these fluorophores typically averages around one nanosecond but varies depending on the type of fluorophore and its microenvironment, such as binding. For example, the reduced coenzyme NADH exhibits fluorescence lifetimes of ~0.2 ns in its free form and 2-3 ns when bound to proteins. Time-correlated single photon counting (TCSPC) allows precise measurement of these lifetimes, and fluorescence lifetime imaging (FLIM) visualizes them as color-coded maps [13].

Preprints.org (www.preprints.org) | NOT PEER-REVIEWED | Posted: 25 December 2024 doi:10.20944/preprints202412.2129.v1

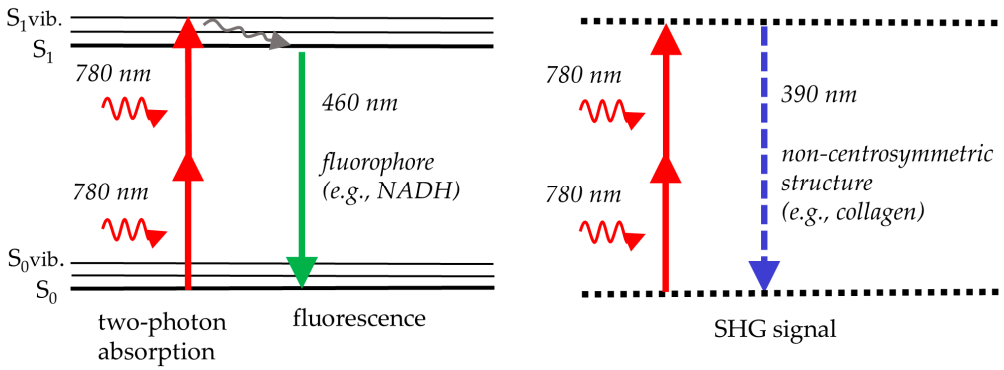

Figure 1. The scheme illustrates two-photon fluorescence, e.g., from NADH, excited with near infrared light at 780 nm (**left**), and second harmonic generation (SHG), e.g., from collagen, at half the laser wavelength (doubling the laser frequency) (**right**). Fluorescence occurs from the lowest vibrational level of the first real electronic state, S_1. In SHG, two photons are upconverted to a single SHG photon by a virtual state of a non-centrosymmetric molecule.

Figure 2 presents a typical AF decay curve and a pseudo-colored FLIM image of the epidermis obtained from a horizontal MPT section. The AF signal generated within the sub-femtoliter two-photon excitation volume of the focusing optics often contains contributions from multiple fluorophores or various binding states, leading to biexponential (or multiexponential) fluorescence decay.

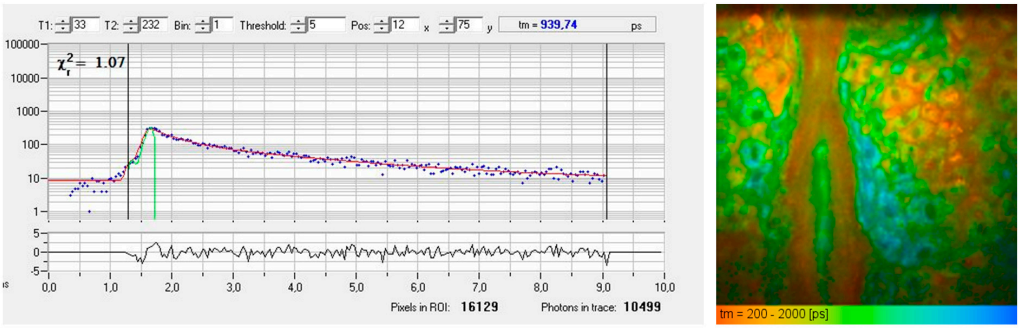

Figure 2. FLIM measurement of the living human epidermis using time-correlated single photon counting (TCSPC). (**Left**) The fluorescence decay curve of a particular pixel illustrates counts of detected fluorescence photons in different time channels (blue dots). A χ^2 value of 1.07 confirms a good fit (red fitting curve) obtained by a biexponential approach with a mean autofluorescence lifetime of 940 picoseconds. (**Right**) The FLIM image shows a color-coded map of fluorescence lifetimes, ranging from 200 ps (red, corresponds to temporal resolution) to 2000 ps (blue).

The MPT device scans the skin and provides non-invasively horizontal and axial optical sections [14]. When equipped with NA1.3 focusing optics, it achieves a lateral resolution better than 0.5 µm and an axial resolution of approximately 2-3 µm. Notably, MPT offers the highest spatial resolution among all skin imaging techniques. With a working distance of 0.2 mm, the entire human epidermis as well as the upper dermis can be imaged with superior resolution in most skin regions (Figure 3).

Preprints.org (www.preprints.org) | NOT PEER-REVIEWED | Posted: 25 December 2024 doi:10.20944/preprints202412.2129.v1

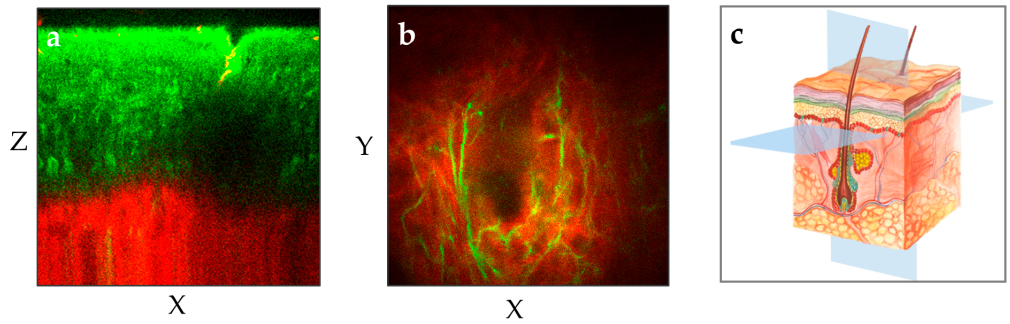

Figure 3. The two MPT images illustrate two different perspectives of the human forearm skin: **(a)** The vertical plane (XZ) provides a cross-sectional view of the skin from the outermost layer *stratum corneum* down to the upper dermis with the red-depicted SHG signal. **(b)** The horizontal "en face" plane (XY) within the upper dermis demonstrates the elastin (green, autofluorescence) and collagen (red, SHG) at a depth of 100 µm. **(c)** The illustration shows the XY and XZ imaging planes in the context of the skin's anatomy.

3. Three Generations of Multiphoton Tomographs

All tomographs are based on a mode-locked near infrared 80 MHz femtosecond laser delivering approximately 500 million laser pulses per optical section with a typical field of view of 0.2x0.2 mm^2 (512x512 pixels) in just 6 seconds. Two or more single photon detectors are employed to realize AF, SHG, and FLIM imaging. Some of the devices are equipped with additional modules to realize (i) Raman imaging by CARS (Coherent anti-Stokes Raman Spectroscopy), (ii) endoscopy, or (iii) RCM imaging.

3.1. DermaInspect

The first generation "*DermaInspect*" was based on a Ti:sapphire femtosecond laser on an optical table. Subjects were positioned beneath the NA1.3 focusing optics adjacent to the optical table [6]. The first prototype was adopted by the cosmetic company Beiersdorf in 2001 (Figure 4). The major innovation was the introduction of an optical arm, along with the add-on two-photon GRIN microendoscope with an outer diameter of 1.2 mm, designed for imaging difficult-to-access skin areas [13].

In part, multiphoton tomographs were upgraded with a spectrometer to realize two-photon fluorescence spectroscopy with high spatial and temporal resolution (spectral FLIM). This enhancement enabled the creation of "5D intravital tomography," incorporating fluorescence lifetime as the fourth dimension and emission spectrum as the fifth. The *DermaInspect* in the *Princess Alexandra Hospital in Brisbane* was equipped with a filter wheel to realize spectral FLIM. Similarly, the *Hammersmith Hospital* in London employed two-photon spectral FLIM [15].

Additionally, *DermaInspect* facilitated imaging of CARS signals, enabling high-resolution visualization of lipids and water in the skin. To achieve that, two laser beams with distinct wavelengths had to be employed. The *DermaInspect-CARS* system combined a Ti:sapphire laser with an optical parametric oscillator (OPO) emitting in the spectral range of 1000 nm to 1300 nm to generate the necessary "Stokes beam". This setup detected the Raman active molecular vibration of CH_2 in lipids at 2845 cm^{-1}, within the red spectral range [16–18].

 doi:10.20944/preprints202412.2129.v1

Figure 4. The first two-photon skin imaging device: multiphoton tomograph. This prototype was delivered to the Beiersdorf AG in Hamburg in 2001.

3.2. MPTflex

The second generation, "MPT*flex*", introduced mobility and a 360° imaging head connected to both a mechanical arm and an articulated optical arm for laser beam transmission. The tunable Ti:sapphire laser and its chiller were housed within the moveable unit.

The MPT*flex*-CARS variant utilized a photonic crystal fiber (PCF) for white-light generation, providing the Stokes beam required for CARS imaging. The two laser beams are guided through the optical arm and overlap in space and time in the sub-femtoliter volume of the NA1.3 focusing optics [16]. Figure 5 shows the MPT*flex* with two photon detectors and MPT*flex*-CARS with four photon detectors.

Figure 5. Multiphoton tomographs MPT*flex* and MPT*flex*-CARS based on a water-chilled tunable femtosecond Ti:sapphire laser, beam delivery through an optical arm, and the 360° imaging head with up to four photon detectors for the measurements of two-photon excited autofluorescence, SHG, and RAMAN/CARS signals of lipids and water.

 doi:10.20944/preprints202412.2129.v1

3.3. MPTcompact

The latest generation MPT*compact* [10] combines five complementary image modalities (i) two-photon AF, (ii) SHG, (iii) FLIM, (iv) RCM, and (v) dermoscopy with a white light CMOS camera. This system employs an ultracompact er-doped femtosecond fiber laser operating at 780 nm directly integrated into the imaging head. An optical arm is no longer required. The *MPTcompact* is designed for unparalleled portability, capable of operating on batteries and charging via flexible solar panels (Figure 6).

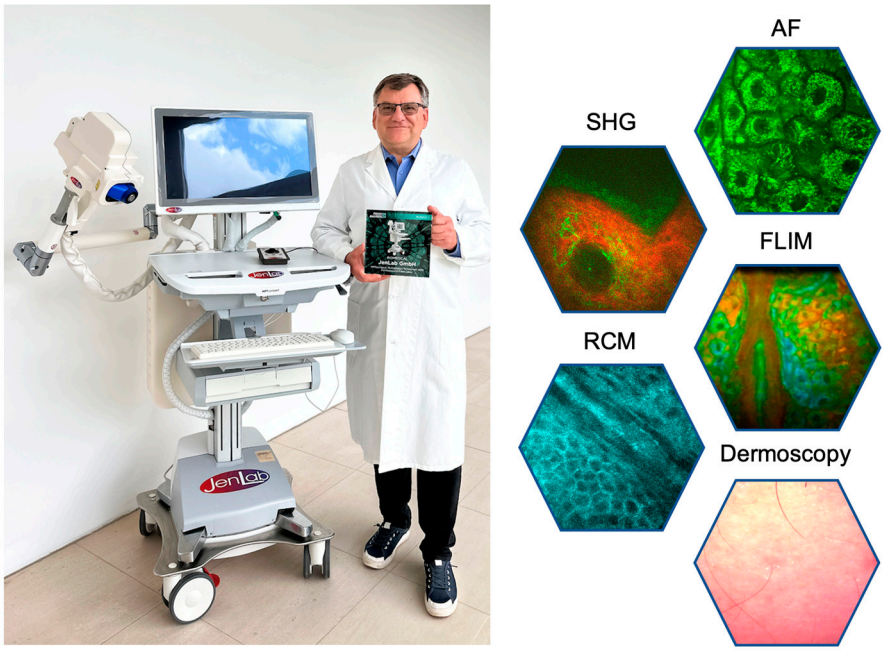

Figure 6. The latest "Prism Award 2024" winning multimodal multiphoton tomograph MPT*compact* with its ultracompact fiber laser head, integrated into the imaging head. The optical arm and the chiller are no longer required. The tomograph can run on batteries.

4. Historical Overview of MPT Studies on Human Volunteers in Cosmetic Research

In 2000, the cosmetic company Beiersdorf AG signed a contract with the start-up company JenLab GmbH to pioneer the first two-photon skin imaging device. The same year, the first prototype of the multiphoton tomograph "*DermaInspect*" was delivered to the Beiersdorf AG headquarters in Hamburg, Germany [15]. Initial applications included investigating the swelling and shrinking effects of the *stratum corneum*, imaging aged skin, and addressing safety considerations [19–22].

In 2002, the first clinical *in vivo* MPT study on 53 patients with melanocytic lesions was performed. Based on this successful clinical study, the CE0118 certificate for the femtosecond laser system *DermaInspect* as medical device was granted by the European Certified Body *Thuringian State Authority of Metrology and Verification (LMET)* in 2004. The multiphoton tomograph *DermaInspect* became the world's first femtosecond laser medical device for nonlinear clinical imaging [15].

In 2005, the *DermaInspect* was employed in a large clinical cosmetic study titled "Investigation of the efficacy of a crème for the care of mature skin. Controlled, randomized, prospective study" and approved by the Ethics Committee. Researchers from JenLab and the University Hospital Jena collaborated with *L'Oreal* to measure dermal extracellular matrix (ECM) modifications in 24 volunteers prior to and after administration of selected plant extracts. MPT measurements were conducted (i) before taking twice a day two anti-aging products, (ii) after 1 month, and (iii) after 3 months of administration. Cream B exhibited a strong effect on the ECM after one month compared

 doi:10.20944/preprints202412.2129.v1

with the untreated skin area and cream A. Bazin et al. stated: “To our knowledge, it is the first time that it was possible to demonstrate *in vivo* the effect of a cosmetic product on the superficial dermal layer, in a non-invasive and non-destructive process, i.e., without cutting the skin” [23].

In 2006, *DermaInspect* facilitated a clinical study involving 18 Caucasian volunteers (7 women and 11 men, aged 21–84 years) at the University Hospital Jena. This research established morphological criteria for skin aging using *in vivo* two-photon imaging of the ECM.

In 2007, ten *DermaInspect* devices were operational in clinics in Germany and Australia as well as within cosmetic research facilities in Germany (*Beiersdorf*) and Japan (*Kao, Shiseido*).

In 2009, the *DermaInspect*-CARS system became the worldwide first certified medical device for CARS imaging (CE0118). Clinical CARS imaging studies were conducted at Charité in Berlin on patients suffering from psoriasis. Distinct lipid distributions on the cellular level were found in patients with psoriasis compared to healthy skin [15].

The next significant milestone was achieved on November 8, 2010, when the MPT*flex* multiphoton tomograph received CE0118 certification as a medical device. The same year, JenLab received in San Francisco the prestigious *Prism Award* for photonic products in Life Sciences. The first multiphoton tomograph MPT*flex* was delivered to the *University Hospital Mannheim* in April 2009. Huck et al. reported [24] the first *in vivo* two-photon FLIM studies ("optical metabolic imaging" OMI) on skin inflammation in patients suffering *from atopic dermatitis (AD*). These studies highlighted significant differences in coenzyme FLIM data between AD-affected and healthy skin, reflecting altered metabolism in the upper epidermal layers.

In 2011, the Beckman Laser Institute at the University of California, Irvine, acquired an MPT*flex* tomograph and initiated studies on melanin distribution, skin physiology, and skin cancer detection. By 2023, the third-generation "MPT*compact*" was launched.

Today, multiphoton tomographs are widely utilized by major cosmetic and pharmaceutical companies to assess anti-aging effects, the intratissue distribution of cosmetic ingredients, product-cell interactions, and skin responses [15].

5. Key Application Fields of MPT in Cosmetic Research

5.1. MPT of Healthy Human Skin

Most MPT measurements of human volunteers are performed on the forearm, using an interface comprising a round coverslip secured by a magnetic metal ring (Figure 7). The interface is taped to the skin and magnetically connected to the tomograph. Typically, a mean laser power of 20 mW is used, which can be increased up to 50 mW for deeper imaging. The dwell time of the focused laser beam is only a few microseconds per pixel. Averaging is not required. AF, SHG, and RCM are recorded simultaneously, with zoom capabilities enabling precise imaging. Horizontal optical sections are usually captured in 5 µm steps along the z-axis.

Measuring the *stratum corneum* is particularly challenging due to motion artifacts and the strong signals from keratin. Breathing artifacts appear as dark "stripes" in the skin surface image (Figure 8). The *s. corneum* is characterized by hexagonal, nucleus-free cells, whereas diseased skin (e.g., psoriasis, eczema, and dermatitis) often exhibits corneocytes with retained nuclei, reflecting disrupted keratinocyte maturation (Figure 8).

Preprints.org (www.preprints.org) | NOT PEER-REVIEWED | Posted: 25 December 2024 doi:10.20944/preprints202412.2129.v1

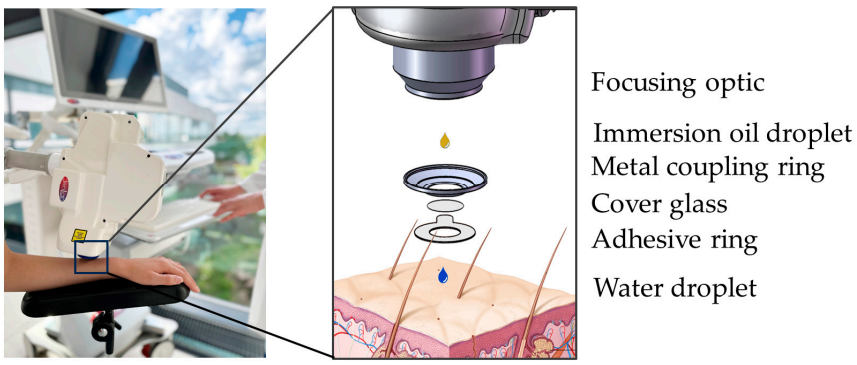

Figure 7. MPT-Interface. Left: The interface "connects" the human subject with the tomograph via magnetic forces (**left**). Detailed schematic view (**right**). The focusing optic is facilitated by an immersion oil droplet for optimal refractive index matching. The metal coupling ring with a cover glass is mounted on an adhesive ring. The round coverslip provides a transparent barrier and, together with a drop of immersion oil, reduces refractive index mismatch. The water droplet avoids air between cover glass and skin and, therefore, enhances image quality.

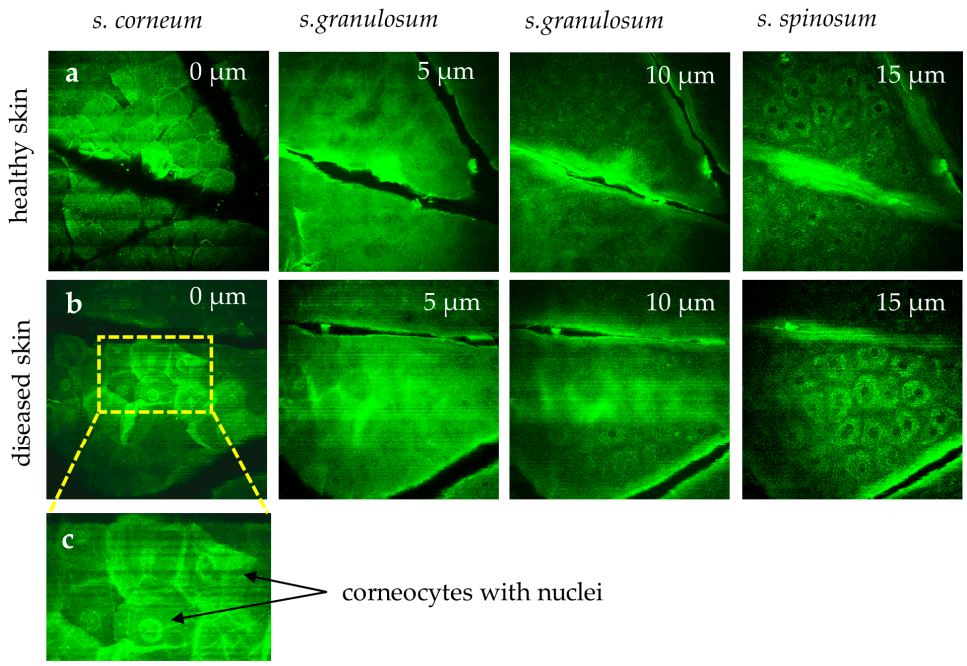

Figure 8. MPT images highlights differences in healthy skin **(a)** versus diseased skin **(b)**. In the healthy *stratum corneum*, polygonal corneocytes lack nuclei. However, in diseased conditions (e.g., psoriasis, eczema, dermatitis), corneocytes **(b)** often retain nuclei, reflecting disrupted keratinocyte maturation. **(c)** The region of interest area highlights corneocytes with retained nuclei. The "stripes" in the first image reflect breathing artifacts.

When going deep, the diffuse fluorescent layer *s. granulosum* becomes visible. Below this, the keratinocytes in the *s. spinosum* display fluorescent mitochondria. The basal layer (*s. basale*) contains melanin, the strongest fluorophore. Finally, the first SHG signals appear on the top of a *dermal papillae*, marking the onset of the epidermal-dermal junction. A typical value for the depth of this junction is between 50 µm and 70 µm for the inner forearm. When going deeper, elastin fibers can be imaged via AF, while SHG reveals the collagen network (Figure 9). Occasionally, fluorescent fibroblasts and mast cells can also be identified. Mast cells are immune cells located within the *papillary dermis* with a typical cell diameter of ten micrometers. Mast cells are inactive in healthy skin but become "activated" during conditions such as inflammation (e.g., *psoriasis, dermatitis, mastocytosis*) [25].

 doi:10.20944/preprints202412.2129.v1

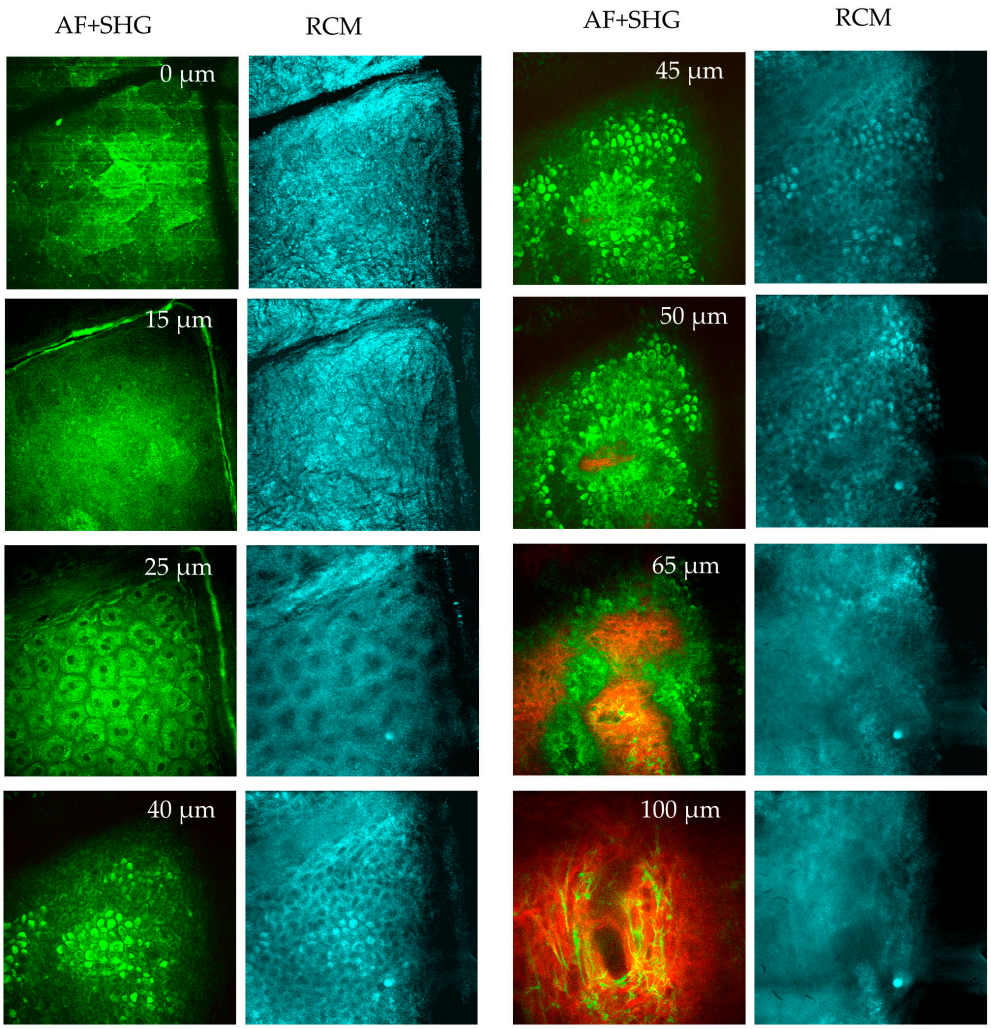

Figure 9. MPT *en face* sections out of a stack of images taken from a human forearm down to a tissue depth of 100 micrometers. Two-photon excited autofluorescence (green) and SHG (red) (overlay), and confocal reflection (RCM, blue) signals are used to visualize the epidermis and upper dermis. At 0 µm depth (*s. corneum)*, the AF image reveals large, polygonal keratinized cells without nuclei. The *stratum corneum* is highly reflective, as seen in the RCM image. Skin folds are evident in both AF and RCM images. At 15 µm depth (*s. granulosum): the* granulated and reflective layer is visible. At 25 µm *(s. spinosum)*, well-defined keratinocytes with bright, grainy fluorescent cytoplasm are seen in the AF images, attributed to organelles such as mitochondria. The dark nuclei lack fluorescence. RCM images show a honeycomb pattern. When imaging at 40-45 µm depth (*s. basale,* melanin-containing cells appear brighter due to the presence of melanin caps above their nuclei. These melanin caps are also visible in RCM images due to the high refractive index of melanin. A little bit deeper at 50 µm (*s. basale),* a mix of AF and SHG signals from collagen structures are recorded. When imaging the upper dermis at a depth of 65 µm (*d. papillae),* pronounced collagen fibers (red, SHG) and cells (green) are seen presenting the epidermal-dermal junction. In a depth of 100 µm (upper dermis), dense collagen fibrils (red) and the elastin networks (green) are seen, as well as a few mast cells.

Forearms are commonly used for MPT studies due to their accessibility, but imaging the face is increasingly of interest. A multiphoton multimodal face imager is under development, and one study has reported on MPT imaging of a 29-year-old female volunteer's eyelid [26]. The measured thickness of the epidermis in the eyelid was found to be 47.1 µm ± 3.6 µm. The FLIM histogram showed a double fluorescence lifetime peak (0.5 ns and 1ns) at an epidermal depth of 15 µm, a single maximum at about 1 ns when 20 µm deep, and 0.5 ns at 45 µm skin depth. It was a challenge to measure the anterior epidermis due to movement artifacts.

 doi:10.20944/preprints202412.2129.v1

MPT has also been employed to study the collagen network in facial skin, without AF imaging, using SHG microscopy alone [27,28]. Additionally, MPT coupled with coherent anti-Stokes Raman scattering (CARS) and stimulated Raman scattering (SRS) can image non-fluorescent molecules like lipids, water, and specific chemicals [16–18,29].

5.2. Optical Metabolic Imaging

Besides the measurement of AF intensity values, FLIM data can be obtained to study intracellular coenzymes. By selecting appropriate laser excitation wavelengths, specific coenzymes can be targeted. At wavelengths above 800 nm, flavins and flavoproteins, such as flavomononucleotide (FMN), exhibit fluorescence lifetimes of approximately 5 ns. However, reduced nicotinamide adenine dinucleotide (NADH) cannot be detected at these excitation wavelengths.

When using excitation wavelengths of 780 nm or less, the reduced coenzyme NADH can be excited, while its oxidized form (NAD^+) remains non-fluorescent. NADH yields stronger fluorescence signals than flavins, with two distinguishable lifetimes: a short component (~0.2 ns) representing free NADH and a long component (~2 ns) indicating protein-bound NADH, such as complexes within the mitochondrial membrane. These characteristics make NADH and flavins robust metabolic indicators, enabling MPT to assess the metabolic state of intratissue cells.

The autofluorescence ratio of NADH to flavin, as well as the ratio of free-to-bound NADH, can be used for optical metabolic imaging (OMI). Also, changes in the mean fluorescence lifetime (τ_m), calculated from amplitudes and lifetimes of the short and long fluorescent components, serve as markers for altered metabolism:

$$\tau_m = (a_1 \tau_1 + a_2 \tau_2) / (a_1 + a_2)$$

For instance, inflamed skin typically shows a shorter mean AF lifetime than surrounding healthy skin [24]. This approach has also differentiated between activated and resting mast cells in the dermis, with activated cells exhibiting significantly shorter lifetimes [25]. A notable application by *L'Oréal* involved studying changes in fluorescent coenzymes under UVA-induced metabolic stress using two-photon FLIM [30,31].

Figure 10 demonstrates AF imaging of a single intratissue cell in the forearm of a female volunteer during oxygen inhalation. Over a two-hour observation, the fluorescence intensity and FLIM values of a specific cell close to a dermal capillary were determined. Significant changes due to the impact of oxygen diffusion were found. Interestingly, the individual intratissue cell could be tracked and imaged without motion artifacts.

 doi:10.20944/preprints202412.2129.v1

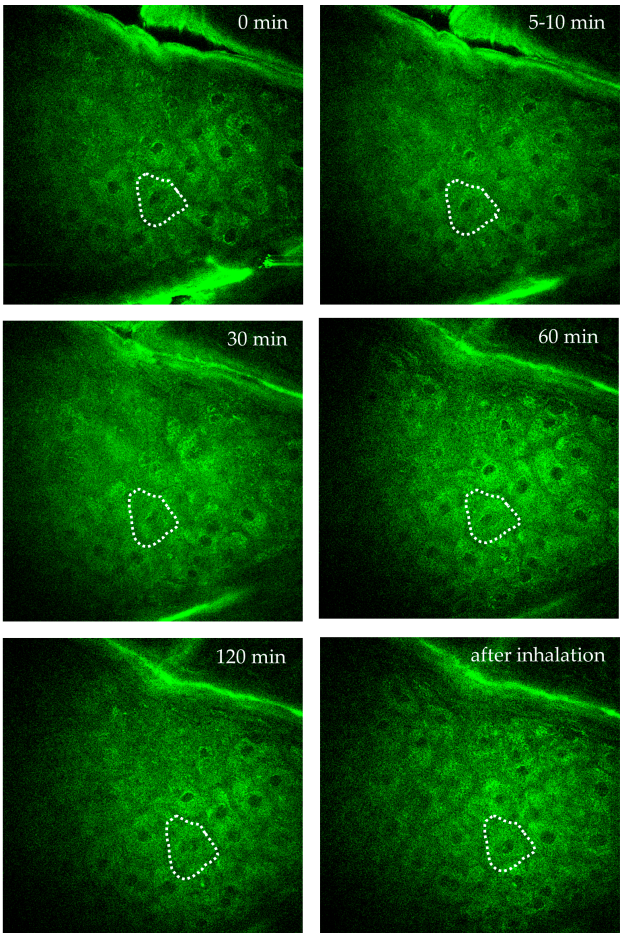

Figure 10. Time-lapse imaging of a single intratissue cell in the *s. spinosum* during oxygen inhalation over 2 hours to monitor intracellular metabolic activity of a specific single cell. The cell is highlighted by the dotted region of interest (ROI). Images were captured at specific time points: before oxygen supply = 0 min, at 5–10 minutes, 30 minutes, 60 minutes, 120 minutes during oxygen inhalation, and after inhalation. The images demonstrate the possibility to track and to image a single intratissue cell over hours without significant motion artefacts.

5.3. Imaging Intratissue Melanin

Melanin, the pigment responsible for skin, hair, and eye color, protects epidermal cells from ultraviolet (UV) radiation. Changes in melanin production induce hyperpigmentation (e.g., sunspots, melasma) or hypopigmentation. Synthetic melanin is commonly used in sunscreens and cosmetic makeup products to mimic its natural properties.

Notably, melanin fluoresces strongly under MPT excitation. The pigment has a broad excitation band and, therefore, allows imaging across the femtosecond Ti:sapphire laser spectrum. Melanosomes in the basal layer, as well as melanocyte dendrites, can easily be visualized.

Figure 11 shows optical FLIM sections of a hyperpigmented spot. The 780 nm excited pigment melanin can be easily depicted in false color-coded FLIM images due to its very short fluorescence lifetime in contrast to the coenzyme autofluorescence. Interestingly, melanin granules are found at different z-depths from nearly the surface (5 µm) down to the epidermal-dermal junction (65 µm).

The cosmetic research is interested to study the effects of solar exposure in dependence on skin phototype, e.g., to understand aged skin, to investigate the efficiency of sunscreens, and to evaluate compounds that modulate melanin synthesis [32–35]. For example, Pena et al. from *L'Oreal* studied *skin whiting* by retinoid-induced decrease in melanin [31]. Retinoids are compounds derived from vitamin A and used in skin care products to improve skin texture and skin tone. They promote cell turnover. Retinoids can also help to treat dark spots and hyperpigmentation.

 doi:10.20944/preprints202412.2129.v1

For instance, Pena et al. from *L'Oreal* used MPT-FLIM to quantify epidermal melanin content in a 12-day study on photodamaged skin treated with retinol (0.3%) and retinoic acid (0.025%). The treatment significantly reduced melanin content and showed anti-aging effects, such as epidermal thickening and enhanced epidermal-dermal junction modulation [31].

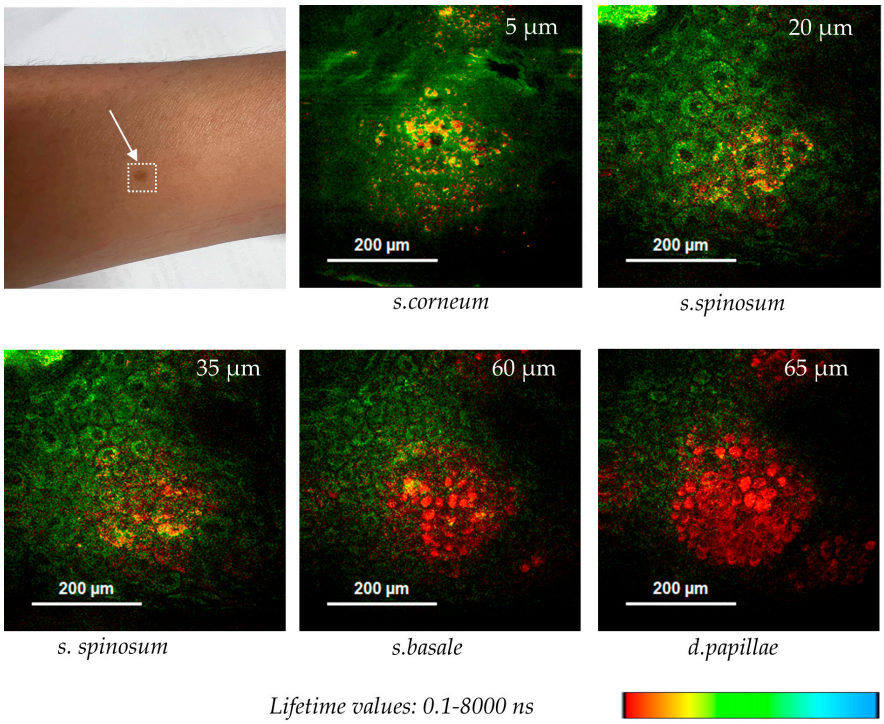

Figure 11. Melanin distribution in a hyperpigmented spot imaged by two-photon FLIM using the multiphoton tomograph MPT*compact*. Melanin with its short autofluorescence lifetime is false color-coded in red, while NADH, with longer AF lifetime values, is false color-coded in green. Melanin granules were found at different z-depths (5 - 65 µm).

MPT also enables imaging of melanin within the hair, a skin appendage emerging from the hair follicle. The hair shaft is a keratinized structure consisting of three layers *(cuticle, cortex, and medulla),* contains two types of melanin: pheomelanin (blond/red hair) and eumelanin (brown/black hair). The ellipsoidal melanin granules have a size of about 0.9 µm x 0.3 µm. The long axis is aligned parallel to cortex fiber.

Interestingly, the two types of melanin *eumelanin* and pheomelanin can be distinguished with special fast FLIM detectors of high temporal resolution. A single photon counting detector is required with a rise time of less than 100 ps. Using high-temporal-resolution FLIM detectors, such as the R3809U-50 MCP with a low time spread of 24 ps, Ehlers et al. [34] distinguished eumelanin's shorter lifetime (40 ps in black hair) from pheomelanin's longer lifetime (340 ps in blond hair). Grey hair, with minimal melanin, exhibited keratin's characteristic fluorescence lifetime (~1.4 ns). FLIM further assists in analyzing artificial hair treatments, such as coloration or bleaching. For example, dyed hair ("Lava red" from *L'Oréal*) was examined with high-temporal-resolution FLIM detectors. Additionally, hair shafts and follicles are studied as potential reservoirs for cosmetic substances.

Beyond cosmetic applications, MPT has investigated pigmented skin lesions (e.g., nevi). Studies, by Lentsch et al., explore malignant melanoma diagnosis by assessing lesion morphology [37].

5.4. MPT Studies on Skin Aging

Epidermal aging involves several structural and functional changes, including thinning of the viable epidermis, reduced melanocyte activity, decreased Langerhans cell density, slower

 doi:10.20944/preprints202412.2129.v1

keratinocyte turnover, and a diminished barrier function. Dermal aging includes about one percent loss of collagen per year by the age of 40, with collagen reduction beginning as early as 25 years of age. Additional changes include a decrease in collagen crosslinks, degradation of elastin fibers, and the resulting formation of fine lines, wrinkles, and dermal thinning. Moreover, hyaluronic acid levels diminish with age, leading to less hydrated and less plump skin. Other age-related effects include reduced fibroblast activity, decreased sebaceous gland function, and a flattening of the epidermal-dermal junction.

To mitigate skin aging, strategies such as consistent sun protection, proper hydration, and the use of anti-aging products containing retinoids, peptides, and antioxidants are recommended. In more advanced cases, interventions like dermal fillers can also be employed to restore volume and structure.

MPT offers the possibility to monitor the skin aging effects including the thinning of the epidermis, modifications of the epidermal-dermal junction, the appearance of age spots, etc. MPT is also used to test the cosmetic-induced collagen synthesis. Interestingly, the ratio collagen to elastin can be used to define a skin age parameter SAAID (SHG-to-Autofluorescence Aging Index of Dermis). This parameter ranges from approximately 0.3 in individuals aged 20 to around -0.3 in individuals aged 70. Effective antiaging interventions can increase the SAAID value, whereas e.g., excessive UV exposure decrease it [38–53]. Leading cosmetic companies, including *Beiersdorf AG*, *L'Oréal,* and *Shiseido*, utilize MPT*flex* systems to evaluate skin-age parameters. These systems allow for in-depth studies of aged skin and the validation of anti-aging effects in their formulations.

5.5. Detection of Antioxidative Means

The antioxidative effects on the skin, particularly their "energizing" impact, can be effectively measured using MPT. MPT enables the detection of changes in coenzyme states, specifically the transition between oxidized and reduced forms. This includes the detection of the oxidized coenzyme NAD, which is non-fluorescent, in contrast to its reduced counterpart, NADH, which exhibits fluorescence.

A study conducted by Miyamoto and Kudoh from *Procter & Gamble* demonstrated a significant correlation between NADH levels in keratinocytes within the epidermal granular layer and factors such as age and skin mechanical elasticity. Their research included both European and Japanese female subjects, providing insights into how NADH levels change with aging and skin condition. They used these MPT findings to evaluate the effect of novel P&G skin care formulations [53].

5.6. Imaging of Nanoparticles in Skin

The use of nanoparticles (NPs) in cosmetics is a growing area of research aimed at reducing the risk of side effects, such as systemic entry into the bloodstream, accumulation in the liver and other organs, and potential cytotoxic effects, including long-term skin inflammation. MPT can provide information on the penetration and accumulation of the nanoparticles as well as to study nanoparticle-cell interactions.

Metallic sunscreen nanoparticles are applied due to their high reflectivity of UV sunlight and their "invisible" appearance. Nanoparticles, such as zinc oxide (ZnO) and titanium dioxide (TiO_2) particles with a size of 20-50 nm are commonly used in sunscreen products. The nano-sized particles have a high efficiency in Rayleigh scattering of UVB and UVA sunlight and, therefore, a high sun protection factor without the undesired whitening effect on the skin.

Despite their benefits, the use of metal oxide nanoparticles in cosmetics remains controversial due to concerns about their potential to penetrate the *s. corneum* and enter the systemic circulation. Furthermore, metal oxides can generate free radicals due to their photocatalytic activity after UV absorption.

 doi:10.20944/preprints202412.2129.v1

However, it was found that TiO_2 particles larger than 30 nm do not penetrate the skin barrier in healthy individuals. The *European Scientific Committee on Cosmetics and Non-Food Products* recommended the use of TiO_2 in cosmetic products in 2000 [54,55].

It should be noted that the resolution of the MPT is about 300 nanometers, which is not sufficient to resolve single NPs if their distance from each other is less than 300 nm. However, a single NPs, as well as clusters of NPs, can be imaged. Interestingly, ZnO particles and clusters are detectable by SHG. Several MPT studies [55–57] have shown that ZnO NPs distribute in the *s. corneum,* as well as in the furrows, wrinkles, and orifice of hair follicles. ZnO nanoparticles at a size of 30 nm do not reach the living epidermis in healthy skin.

Beyond sunscreens, engineered nanoparticles are increasingly used in skin care products to enhance the delivery and efficacy of active ingredients. Nanocarriers such as liposomes and polymeric nanoparticles encapsulate antioxidants and moisturizing agents, allowing them to penetrate the skin barrier and deliver actives to targeted layers or cells. Encapsulation also protects against rapid degradation of these ingredients [58,59]. Hair follicles are being explored as potential long-term reservoirs for nanoparticles, making this an intriguing research focus.

MPT has also been used to investigate tattoo pigments, which consist of micro- and nanoparticles. König performed the first MPT studies on intratissue tattoo particles [60]. "UV tattoos" that fluoresce under femtosecond NIR laser exposure were examined. Metallic and non-centrosymmetric tattoo nanoparticles can be visualized using second harmonic generation (SHG) imaging. In cases where tattoo dyes are fluorescent, fluorescence lifetime imaging microscopy (FLIM) enables the differentiation of particle types and discrimination between endogenous fluorophores and cosmetic ingredients. Recently, Ngyen et al. reported on MPT studies on intratissue tattoos [61]. Kröger et al have shown in their MPT studies that the uptake of tattoo nanoparticles by Langerhans cells and macrophages can be visualized by two-photon excited fluorescence of endogenous fluorophores as well as of the tattoo pigments. The intracellular accumulation of tattoo nanoparticles allows imaging of Langerhans cells, which are otherwise challenging to detect via two-photon excitation [62].

The contamination of skin products with micro- and nanoplastics is a pressing environmental and health concern. Current methods to detect these particles are e.g., RAMAN spectroscopy, mass spectroscopy, and fluorescence detection after staining. We found that many plastic materials exhibit a significant AF when excited with UV light. Therefore, a novel approach to image plastic microparticles and nanoparticles is to use two-photon excited autofluorescence. Anilkumar et al. demonstrated that MPT can detect autofluorescent plastic microparticles in human skin *in vivo*, offering a novel approach for studying plastic contamination in cosmetics (Figure 12) [63].

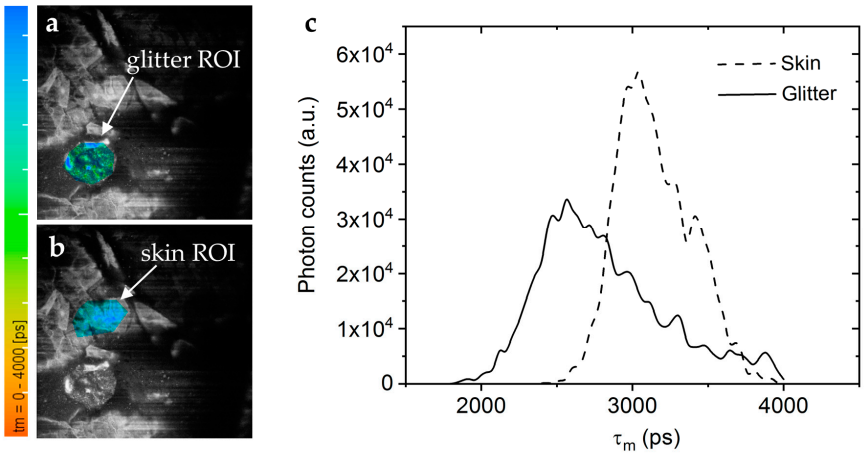

Figure 12. Microplastics in decorative cosmetic formulations were *in vivo* tracked in human skin using FLIM. **(a)** The FLIM of the blue/green region of interest (ROI) highlights the microplastic particle localized in the *s. corneum*.

 doi:10.20944/preprints202412.2129.v1

(b) A second "Glitter-free" blue ROI shows the surrounding skin autofluorescence for comparison. The color scale represents the mean fluorescence lifetime values from 0 – 4000 ps. **(c)** The FLIM histogram shows that the microplastic particle (solid line) has a nearly 0.5 ns shorter mean lifetime than the surrounding skin tissue (dashed line).

5.7. Imaging of Topically Applied Cosmetics and Pharmaceuticals

MPT has proven to be a valuable tool for studying the time-lapsed distribution of topically applied substances in the skin. In particular, the tomographs MPT*flex* and MPT*flex*-CARS with their tunable femtosecond laser source have been widely used for intratissue drug detection and analysis of cosmetic agent distribution [e.g., 65-70]. Tuning the laser excitation wavelength is particularly advantageous when targeting exogenous fluorophores that can be excited at higher wavelengths, thereby reducing interference from the skin's autofluorescence and achieving a higher signal-to-noise ratio. Additionally, FLIM can help to distinguish between endogenous and exogenous fluorophores.

In 2018, Alex et al. from GSK reported [67] on a phase I clinical trial, where the spatial distribution and residency of the drug GSK2894512 within the epidermis and dermis of six healthy volunteers was investigated using MPT*flex*-CARS with FLIM module. Two topical drug formulations were applied to the forearms for 7 consecutive days, followed by daily MPT measurements for one week down to a depth of 200 micrometers. In addition, a few punch biopsies were obtained for comparison with MPT results using liquid chromatography-tandem mass spectroscopy. Interestingly, the drug GSK2894512 developed for treating atopic dermatitis and psoriasis showed fluorescence that could be used to track the drug by FLIM. FLIM enabled differentiation between the pharmaceutical ingredient (with a fluorescence lifetime of ~3 ns) and endogenous fluorophores, such as NADH and flavins. The results produced 3D maps of the drug's spatial distribution and residency over time, down to a depth of 60 μm. The highest intratissue drug signal was observed on days 6–7, with approximately 200 ng of drug per gram of skin. By the second post-treatment day, the concentration had declined to near the detection limit of 25 ng/g. This study demonstrated that MPT could significantly reduce clinical trial size, costs, and the burden on volunteers, minimizing the need for invasive biopsies by providing accurate non-invasive measurements.

Bhardwaj et al. from *Colgate-Palmolive* [69] used MPT*flex* to evaluate a novel chemical peeling agent designed for managing facial hyperpigmentation. The study involved nine volunteers and aimed to assess a new peeling formulation free of controversial substances like hydroquinone and trichloroacetic acid, which are known to cause side effects such as inflammation. Three MPT imaging sessions conducted before and after two peeling treatments revealed that the peeling agent reduced melanin concentration while increasing keratinocyte metabolic activity. Importantly, no intratissue signs of inflammation were detected, highlighting the safety and efficacy of the formulation.

The novel multiphoton tomograph MPT*compact* can be also widely used in cosmetic research to understand the accumulation of topically applied substances in the *stratum corneum*, penetration characteristics, and the interaction with the living epidermis. The tomograph has the disadvantage that it is not tunable. However, as shown in Figure 13, topically applied skin care products can be imaged by the multimodal approach including SHG imaging, FLIM, and confocal reflectance imaging.

 doi:10.20944/preprints202412.2129.v1

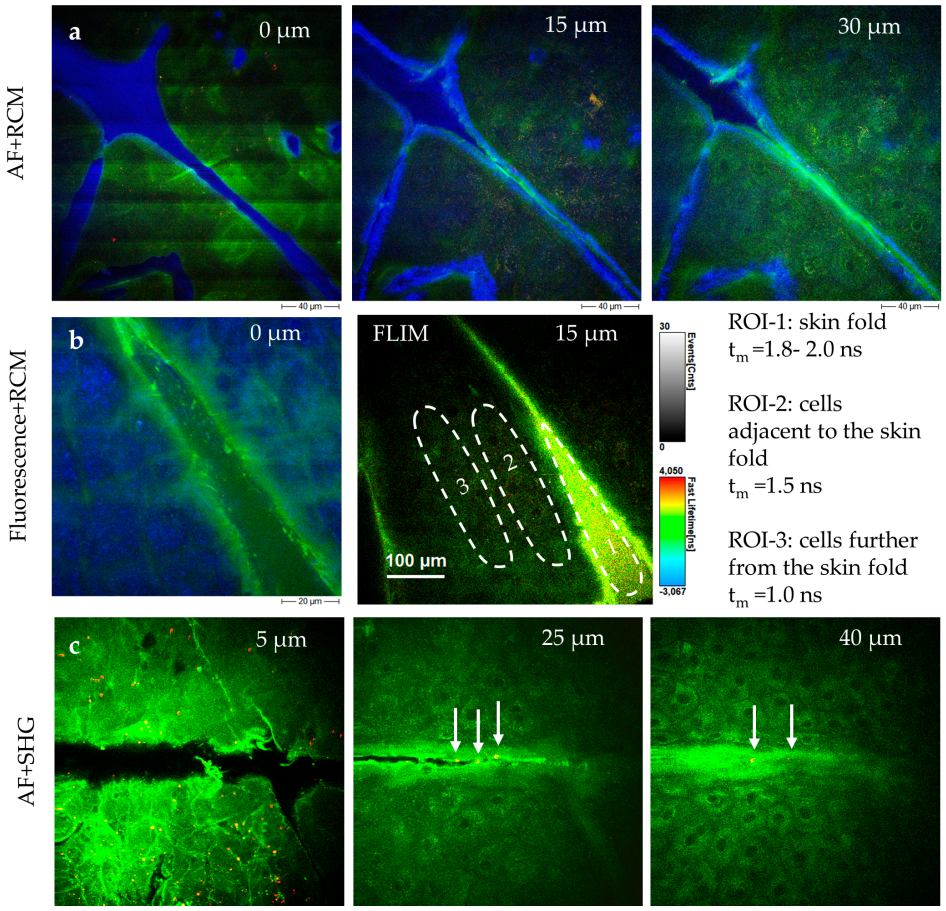

Figure 13. MPT sections demonstrating the possibility of imaging cosmetics *in situ* in human skin with high submicron resolution. **(a)** AF+RCM images of a skin gel (*Gel No. 6 Skin Equalizer, Premium Aesthetic GmbH, Germany*). The strong blue RCM signal indicates an accumulation of the product particularly in skin wrinkles. **(b)** The FLIM images of a skin repair creme (*Ultra Intense Hyaluronic Age Repair Cream, Dr. Joseph GmbH, Italy*) reveal differences in the distribution of the creme and its impact on skin cell metabolism. The false-color coded images represent fluorescence lifetime values (0–4 ns), while the grayscale intensity scale corresponds to photon events. **(c)** AF+ SHG imaging of a creme with collagen components (*ActiVLayr® Premium Skin-Tight Real Collagen Film, DERMA Layr® Technology Inside*). SHG signals (red) visualize the collagen distribution of collagen particles.

5.8. Imaging of Effects of Cosmetic Laser Exposure

"Destructive" lasers are used in cosmetic skin care applications, such as skin resurfacing, tattoo removal, and the treatment of pigmented lesions. Laser-induced skin rejuvenation is based on the generation of micro lesions surrounded by unaffected tissue through exposure to intense laser "microbeams". The micro lesions trigger the formation of new collagen during the repair process in the dermis. Typically, this procedure is done using fractionated laser exposure that is achieved by beam scanning or by the generation of laser beamlets [71]. CO_2 lasers operating at a 1064 nm wavelength are frequently employed in these procedures. Chopped continuous-wave lasers and Q-switched lasers in the nanosecond range have been traditionally used. Depending on the target size and the thermal diffusion time, respectively, the pulse length of the Q-switched laser must be varied to optimize the destruction effects of the target while minimizing thermal damage to surrounding tissue. This process is called selective thermolysis [72].

Relatively new is the application of destructive ultrashort lasers, including picosecond and femtosecond lasers, in cosmetics. These lasers are based on mode-locking. So far, picosecond lasers have been introduced in cosmetics for tattoo removal and the treatment of pigmented lesions, lentigines, melasma, scars, wrinkles, and photodamaged skin [73]. Also, skin rejuvenation can be

 doi:10.20944/preprints202412.2129.v1

done with fractionated non-ablative picosecond lasers. The ultrashort pulses delivered by picosecond lasers generate high peak power for an extremely brief duration, facilitating **laser-induced optical breakdown (LIOB).** This process creates microdamage zones, such as vacuoles, in the skin, which promote subsequent collagen formation. Traditional studies of LIOB effects and the resulting tissue repair relied on biopsies and histochemical analysis.

Balu et al. demonstrated the potential of MPT as a non-invasive, pain-free, and rapid method to study laser-skin interactions and repair mechanisms over time. Using the MPT*flex*, they monitored the effects of picosecond Nd:YAG laser treatments (450 ps pulses at 1064 nm with 3 mJ pulse energy, and 375 ps pulses at 532 nm with 1.5 mJ pulse energy, PicoWay Resolve, Candela) *in vivo* over one month. LIOB-damaged individual cells were visualized 3 hours after exposure. It was found, that melanin-containing cells were significantly damaged, suggesting, that melanin is the primary LIOB target. Later, clusters of cellular necrotic debris were detected in the epidermis. Epidermal microinjuries caused by 532 nm exposure were approximately twice the size of those caused by 1064 nm exposure, with damage zones ranging between 45–60 μm for the latter wavelength. As demonstrated in this pilot study, MPT can characterize laser-induced tissue interactions and post-treatment effects without requiring physical biopsies. [74].

6. The Role of Artificial Intelligence (AI) in Enhancing MPT Image Acquisition and Processing

AI in skin imaging is used to support the diagnosis of skin diseases such as *acne vulgaris* and skin cancer. Traditional applications typically involve the processing of 2D surface images acquired via photography or dermoscopy.

In dermatology, AI employs techniques like convolutional neural networks (CNNs) for pattern recognition and image segmentation. Serna et al. described the segmentation of melanocytes in engineered skin using attribute profiles and area stability approaches [75]**.** Generative adversarial networks (GANs) are also employed for data validation, enabling tasks such as digital staining to mimic conventional H&E histological and immunohistochemical staining, thereby assisting dermatopathologists in interpreting virtual optical biopsies [76].

The use of AI in MPT remains in its early stages but includes digital staining [76], automatic image processing, that reduces manual intervention in data analysis [77], and pattern recognition for disease diagnosis of skin diseases [78–82], in particular black skin cancer (malignant melanoma). Guimaraes et al. used 3663 MPT images with morphological and metabolic information using CNNs for an automatic image processing approach [78]. Prinke et al. utilized segmentation methods to train their networks on MPT image stacks from both healthy and melanoma-affected skin tissue, achieving a diagnostic accuracy of 97% [79]. Lange et al. reported on AI based analysis of MPT images of patients with suspicious pigmented lesions [80].

To our knowledge, there are no publications concerning AI-MPT applications in cosmetics. However, AI could significantly impact this field, focusing on two major goals. First, to enable faster acquisition of optical skin biopsies and second, to analyze MPT data sets regarding quantitative imaging, intratissue tracing of cosmetics, the 3D structure of the elastin-collagen-network, as well as assessment of metabolic activity changes induced by cosmetics.

At JenLab in Berlin, research is underway to accelerate MPT image acquisition using AI. Traditionally, a high-resolution 512x512 pixel AF, SHG and FLIM images, covering a 0.2 mm x 0.2 mm field of view, is acquired in 6 seconds without averaging. The image has a high contrast, requires no further correction such as noise subtraction, and can immediately save as TIFF image. Collecting a stack of 31 optical sections at 5 μm axial steps (covering a skin depth of 0–150 μm) takes approximately 3 minutes.

AI reduces acquisition time by learning cell features and noise levels from existing data and applying this knowledge to rapidly captured images. Using AI, image acquisition can be accelerated sixfold, reducing the time required for one optical section from 6 seconds to 1 second. Consequently,

 doi:10.20944/preprints202412.2129.v1

a stack of 31 optical sections can be acquired in just 30 seconds. AI with "denoising" features further improves the image quality by training on datasets of 6s-skin images vs. 1s-skin images of the same skin location (Figure 14). AI can also enable the easy transition from qualitative MPT image to quantitative analysis, offering insights into intratissue tracing of cosmetics, 3D structural visualization of skin components, and measurement of metabolic changes induced by topical applications [81,82].

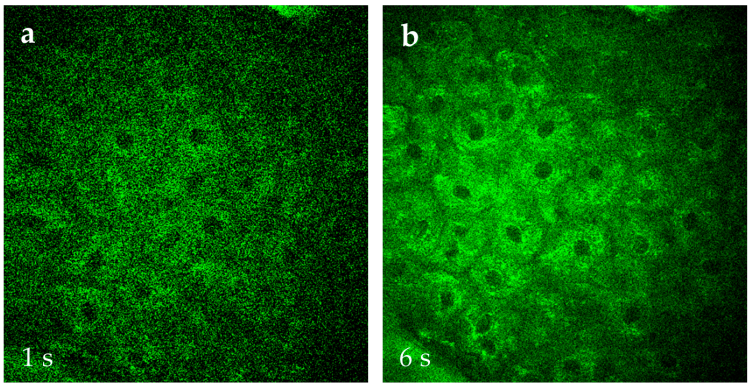

Figure 14. Comparison of AF images of *s. spinosum* cells captured at 1 second scan time per 512x512 pixel frame **(a)** versus 6 seconds **(b)** that is typically used in MPT. The image quality with the preferred faster capture time can be significantly improved when employing AI, e.g., for "denoising".

5. Summary and Conclusions

In cosmetic research, traditional evaluations of "before" and "after" photographs provide surface-level insights into treatment efficacy. However, there is a growing need to gain detailed information on the intratissue distribution of cosmetic compounds and their effects on the living epidermis and extracellular matrix. Importantly, this data should be obtained non-invasively and without the use of animal models.

Historically, the gold standard for skin diagnostics has been histopathology, which involves the microscopic examination of intratissue cells. This requires an invasive procedure. Typically, a physical skin biopsy with a minimum diameter of 3 millimeters (punch biopsy) is extracted from the human body and prepared for examination under a light microscope. More enhanced histochemical analysis is called immunohistochemistry where antibodies connected to exogenous fluorophores are employed to label specific cellular structures, including the cell's cytoskeleton and ECM components such as elastin.

In contrast, **multiphoton tomography (MPT)** offers a non-invasive, high-resolution imaging alternative. This technology enables virtual histopathology in the native tissue environment, eliminating the need for physical biopsies. MPT enables virtual biopsies with a thickness of 2–3 µm and lateral resolution as fine as 300 nanometers, making it a powerful tool for imaging undisturbed skin.

MPT, based on femtosecond laser technology, is widely used for skin disease detection and by leading cosmetic companies across Europe, Asia, and the US [83,84]. Applications in f cosmetic research include the measurement (i) anti-aging effects, (ii) the modifications to the epidermal redox state, and (iii) the evaluation of sunscreen ingredients, including nanoparticles. Nanoparticles in skin care products hold great promise, but their safety is still an area of active investigation. Regulatory bodies, such as the EU Cosmetics Regulation and FDA, mandate comprehensive safety assessments prior to human use.

Typical MPT studies in cosmetic research last from a few hours to measure the immediate effects of the cell's metabolism up to three months when evaluating ECM modifications in the upper dermis.

 doi:10.20944/preprints202412.2129.v1

One of MPT's unique capabilities is tracking individual cells within the skin and recording their metabolic activity through two-photon FLIM.

Further advancements in MPT imaging include expanding the field of view, as demonstrated by Fast et al. [85]. Future technical developments may incorporate the use of special fiber optics for transmitting femtosecond laser pulses to develop even smaller imaging heads and flexible multiphoton endoscopes.

A particularly exciting application of MPT is the evaluation of skin architecture and metabolism at an individual level, paving the way for HighTech personalized skincare solutions. This approach holds the potential to revolutionize how skincare products are developed and tailored to meet the specific needs of individual users.

Author Contributions: Both authors have written, read, and agreed to the published version of the manuscript.

Funding: This review received no external funding.

Data Availability Statement: Data available in cited papers.

Conflicts of Interest: Author Karsten König is the founder of the company JenLab GmbH. The authors declare that the research was conducted without any commercial or financial relationships that could be construed as a potential conflict of interest.

Abbreviations

The following abbreviations are used in this manuscript:

AF	Autofluorescence
AI	Artificial Intelligence
CARS	Coherent anti-Stokes Raman Spectroscopy
CNN	Convolutional neuronal networks
ECM	Extracellular matrix
Er-doped	Erbium-doped
FAD	Flavin adenine dinucleotide
FLIM	Fluorescence lifetime imaging
FMN	Flavomononucleotide
fs	femtosecond
GAN	Generative adversarial network
LIOB	**Laser-induced optical breakdown**
MPT	Multiphoton tomography
NA	Numerical aperture
NADH	Nicotinamide adenine dinucleotide
NIR	Near infrared
NP	Nanoparticle
ns	nanosecond
OCT	Optical coherence tomography
OMI	Optical metabolic imaging
OPO	Optical parametric oscillator
PAT	Photoacoustic tomography
ps	picosecond
RCM	Reflectance confocal microscopy
SAAID	SHG-to-Autofluorescence Aging Index of Dermis
SHG	Second harmonic generation
SRS	Stimulated Raman spectroscopy
TCSPC	Time correlated single photon counting
TiO_2	Titanium dioxide
Ti:sapphire	Titanium sapphire
UV	Ultraviolet
ZnO	Zink oxide

References

1. Huang, D.; Swanson, E.A.; Lin, C.P.; Schuman, J.S.; Stinson, W.G.; Chang, W.; Hee, M.R.; Flotte, T.; Gregory, K.; Puliafito, C.A.; Fujimoto, J.G. Optical coherence tomography. *Science* **1991**, *254*, 1178–1181. DOI: 10.1126/science.1957169.
2. Tsugita, T.; Iwai, T. Optical coherence tomography using images of hair structure and dyes penetrating into the hair. *Skin Res. Technol.* **2014**, *20*, 389–398. DOI: 10.1111/srt.12129.
3. Alex, A.; Weingast, J.; Weinigel, M.; Höfer, M.; Nemecek, R.; Binder, M.; Pehamberger, H.; König, K.; Drexler, W. Three-dimensional multiphoton/optical coherence tomography for diagnostic applications in dermatology. *J Biophotonics* Published online June **2012**. DOI: 10.1002/jbio.201200085.
4. Ying, Y.; Zhang, H.; Lin, L. Photoacoustic Imaging of Human Skin for Accurate Diagnosis and Treatment Guidance. *Optics* **2024**, *5*(1), 133-150. DOI: 10.3390/opt5010010.
5. Braghiroli, N.F.; Sugerik, S.; Freitas, L.A.R.; Oliviero, M.; Rabinovitz, H. The skin through reflectance confocal microscopy — Historical background, technical principles, and its correlation with histopathology. *An. Bras. Dermatol* **2022,** *97*, 697-703. DOI: 10.1016/j.abd.2021/10.010.
6. König, K.; Riemann, I. High-resolution multiphoton tomography of human skin with subcellular spatial resolution and picosecond time resolution. *Journal Biomedical Optics* **2003,** *8*, 432-439. DOI: 10.1117/1.1577349.
7. Goeppert-Mayer, M. *Über Elementarakte mit zwei Quantensprüngen*. *Annalen der Physik*. **1931,** *9*, 273–294. DOI: 10.1002/andp.19314010303.
8. Kaiser, W. The long journey to the laser and its use for nonlinear optics. In K. König (Ed.), *Multiphoton microscopy and fluorescence lifetime imaging: Applications in biology and medicine* Germany: De Gruyter. **2018,** 17-22. DOI: 10.1515_9783110429985-004.
9. Denk, W.; Strickler, J. H.; Webb, W.W. Two-photon laser scanning fluorescence microscopy. *Science* **1990,** *248*, 73–76. DOI: 10.1126/science.2321027.
10. König, K. Multimodal Multiphoton Tomography with a Compact Femtosecond Fiber Laser. *Journal of Optics and Photonics Research* **2024**, 1(1). DOI:10.47852/bonviewJOPR32021730
11. Breunig, H.G.; Studier, H.; König, K. Multiphoton excitation characteristics of cellular fluorophores of human skin in vivo. *Optics Express* **2010,** *18*, 7857-7871. DOI 10.1364/OE.18.007857.
12. König, K.; Schenke-Layland, K.; Riemann, I.; Stock, U.A. Multiphoton autofluorescence imaging of intratissue elastic fibers. *Biomaterials* **2005,** 26, 495-500. DOI:10.1016/j.biomaterials.2004.02.059.
13. König, K. Review: Clinical in vivo multiphoton FLIM tomography. *Methods Appl. Fluoresc*. **2020**, *8*, 034002. DOI:10.1088/2050-6120/ab8808.
14. Breunig, H.G.; Batista, A.; König, K. Vertical Multiphoton Imaging of Human Skin in vivo. *J Clin Med Img* **2022,** *V6*, 1-7.
15. König K. Review: history of multiphoton tomography. SPIE-Proc. **2023,** 123840F. DOI: 10.1117/12.2650485.
16. Breunig, H.G.; Weinigel, M.; Bückle, R.; Kellner-Höfer, M.; Lademann, J.; Darvin, M.E.; Sterry, W.; König, K. Clinical coherent anti-stokes Raman scattering and multiphoton tomography of human skin with femtosecond laser and photonic crystal fiber. *Laser Physics Letters* **2013,** *10*, 025604. DOI: 10.1088/1612-2011/10/2/025604.
17. Weinigel, M.; Breunig, H.G.; Lademann, J.; König, K. In vivo histology: optical biopsies with chemical contrast using multiphoton/CARS tomography. *Laser Phys Lett* **2014,** *11*, 055601. DOI: 10/1088/1612-2011/11/5/055601.
18. König, K.; Breunig, H.G.; Batista, A.; Schindele, A.; Zieger, M.; Kaatz, M. Translation of two-photon microscopy to the clinic: multimodal multiphoton CARS tomography of in vivo human skin. *J. Biomed. Opt*. **2020,** *25*, 014515. DOI: 10.1117/1.JBO.25.1.014515.
19. Richter, T.; Peuckert, C.; Sattler, M.; König, K.; Riemann, I.; Hintze, U.; Wittern, K.P.; Wiesendanger, R.; Wepf, R. Dead but highly dynamic – the stratum corneum is devided into three hydration zones. *Skin Pharmacol Physiol* **2004,** *17*, 246-257. DOI:10.1159/000080218

20. Fischer, F.; Volkmer, B.; Puschmann, S.; Greinert, R.; Breitbart, W.; Kiefer, J.; Wepf, R. Characterization of multiphoton laser scanning device optical parameters for image restoration. *Femtosecond Laser Applications in Biology* **2004,** 5463, 140-145. DOI: 10.1117/12.545604.
21. Fischer, F.; Volkmer, B.; Puschmann, S.; Greinert, R.; Breitbart, W.; Kiefer, J.; Wepf, R. Risk estimation of skin damage due to ultrashort pulsed, focused near-infrared laser irradiation. *Journal of Biomedical Optics* **2008,** 13 (4), 041320-041320-8. DOI: 10.1117/1.2960016.
22. Fischer, F.; Volkmer, B.; Puschmann, S.; Greinert, R.; Breitbart, W.; Kiefer, J.; Wepf, R. Assessing the risk of skin damage due to femtosecond laser irradiation. *Journal of Biophotonics* **2008,** 1 (6), 470-477. DOI: 10.1002/jbio.200810050.
23. Bazin, R.; Flament, F.; Colonna, A.; Le Harzic, R.; Bückle, R.; Piot, B.; Laizé, F.; Kaatz, M.; König, K.; Fluhr, J.W. Clinical study on the effects of a cosmetic product on dermal extracellular matrix components using a high-resolution multiphoton tomograph. *Skin Res Tech* **2010,** *16,* 305-310 DOI: 10.1111/j.1600-0846.2010.00432.x
24. Huck, V.; Gorzelanny, C.; Thomas, K.; Getova, V.; Niemeyer, V.; Zens, K.; Unnerstall, T.R.; Feger, J.S.; Fallah, M.A.; Metze, D.; Ständer, S.; Luger, T.A.; König, K.; Mess, C.; Schneider, SW. From morphology to biochemical state-intravital multiphoton fluorescence lifetime imaging of inflamed human skin. *Sci. Rep.* **2016,** *6,* 22789. DOI: 10.1038/srep22789.
25. Kröger, M.; Scheffel, J.; Nikolaev, V.V.; Shirshin, E.A.; Siebenhaar, F.; Schleusener, J.; Lademann, J.; Maurer, M.; Darvin, M.E. In vivo non-invasive staining-free visualization of dermal mast cells in healthy, allergy and mastocytosis humans using two-photon fluorescence lifetime imaging. *Scientific Reports* **2020,** *10,* 14930. DOI: 10.1038/s41598-020-71901-2.
26. Batista, A.; Breunig, H.G.; Uchugonova, A.; König, K. In vivo multiphoton imaging of the eyelid skin. Proc. SPIE **2017,** *10037,* 100370E-1. DOI: 10.1117/12.2251949.
27. Ogura, Y; Tanaka, Y; Ymashita, T; Yasui, T. Texture analysis of second-harmonic-generation images for quantitative analysis of reticular dermal collagen fibre in vivo in human facial cheek skin. *Experimental Dermatol* **2018**. DOI: 10.1111/exd.13560.
28. Ogura, Y.; Atsuta, K.; Hase, E.; Minamikawa, T.; Yasui. T. Photonic-Crystal-Fiber-Coupled, Hand-Held, Polarization-Resolved Second-Harmonic-Generation Microscope for In Vivo Visualization of Dermal Collagen Fibers in Human Skin. *IEEE Journal of Selected Topics in Quantum Electronics* **2019,** *25,* 1. DOI: 10.1109/JSTQE.2018.2865779, **25**, 1, (1-7), (2019)
29. Saar, B.G.; Freudiger, C.W.; Reichmann, J.; Stanley, C.M.; Holtom, G.R.; Xie, X.S. Video-Rate Molecular Imaging *In Vivo* with Stimulated Raman Scattering. *Science* **2010,** *3.* DOI: 10.1126/science.1197236.
30. Ung, T.; Lim, S.; Solinas, X.; Mahou, P.; Chessel, A.; Marionnet, C.; Bornschlögl, T.; Beaurepaire, E.; Bernerd, F.; Pena, A.M.; Stringari, C. Simultaneous NAD(P)H and FAD fluorescence lifetime microscopy of long UVA–induced metabolic stress in reconstructed human skin. *Scientific Reports* **2021,** 11(1). DOI: 10.1038/s41598-021-00126-8.
31. Pena, A.M.; Decencière, E.; Brizion, S.; Victorin, S.; Koudoro, S.; Baldeweck, T.; Tancrède-Bohin, E. Multiphoton FLIM in cosmetic clinical research. In K. König (Ed.), *Multiphoton microscopy and fluorescence lifetime imaging: Applications in biology and medicine*. De Gruyter. **2018,** 369-393. DOI: 10.1515/9783110429985-021.
32. Pena, A.M.; Decencière, E.; Brizion, S.; Victorin, S.; Koudoro, S.; Baldeweck, T.; Tancrède-Bohin, E. Multiphoton FLIM in cosmetic clinical research. In K. König (Ed.), *Multiphoton microscopy and fluorescence lifetime imaging: Applications in biology and medicine.* De Gruyter. **2018,** 369-393. DOI: 10.1038/s41598-021-03114-0.
33. Pena, A.M.; Ito, S.; Bornschlögl, T.; Brizion, S.;Wakamatsu, K.; Del Bino, S. Multiphoton FLIM analyses of native and UVA-modified synthetic melanins. *International Journal of Molecular Sciences* **2023,** *24*, 4517. DOI: 10.3390/ijms24054517.
34. Ehlers, A.; Riemann, I.; Stark, M.; König, K. Multiphoton fluorescence lifetime imaging of human hair. *Microscopy Research and Technique* **2007,** *70,* 154-161. DOI: 10.1002/jemt.20395.

35. Dancik, Y., Favre, A., Loy, C. J., Zvyagin, A. V.,& Roberts, M.S. Use of multiphoton tomography and fluorescence lifetime imaging to investigate skin pigmentation in vivo. Journal of Biomedical Optics. **2013,** *18(2),* 026022. DOI: 10.1117/1.JBO.18.2.026022.
36. Lentsch, G.; Valdebran, M.; Saknite, I.; Smith, J.; Linden, K.G.; König, K.; Barr, R.J.; Harris, R.M.; Tromberg, B.J.; Ganesan, A.K.; Zachary, C.B.; Kelly, K.M.; Balu, M. Non-invasive optical biopsy by multiphoton microscopy identifies the live morphology of common melanocytic nevi. *Pigment Cell Melanoma Res* **2020,** *33,* 869-877, doi:10.1111/pcmr.12902.
37. Lentsch G.; Balu, M.; Williams, J.; Lee, S.; Harris, R.M.; König, K.; Ganesan, A.; Tromberg, B.J.; Nair, N.; Santhaman, U.; Misra, M. In vivo multiphoton microscopy of melasma. *Pigment Cell Melanoma Res* **2018,** *32,* 403-411, doi: 10.1111/pcmr.12756.
38. Köhler, M.J.; König, K.; Elsner, P.; Bückle, R.; Kaatz, M. In vivo assessment of human skin aging by multiphoton laser scanning tomography. *Optics Letters* **2006,** *31(19),* 2879-81. DOI: 10.1364/OL.31.002879.
39. Köhler, M.J.; Hahn, S.; Preller, A.; Elsner, P.; Ziemer, M.; Bauer, A.; König, K.; Bückle, R.; Fluhr, J.W.; Kaatz, M. Morphological skin ageing criteria by multiphoton laser scanning tomography: non-invasive in vivo scoring of the dermal fibre network. *Exp Dermatol* **2008,** *17(6),* 519-523. DOI: 10.1111/j.1600-0625.2007.00669.x.
40. Köhler, M.J.; Preller, A.; Elsner, P.; Kindler, N.; König, K.; Bückle, R.; Kaatz, M. Intrinsic, solar and sunbed-induced skin aging measured in vivo by multiphoton laser tomography and biophysical methods. *Skin Res Tech* **2009,** *15,* 357-363 / DOI 10.1111/j.1600-0846.2009.00372.x
41. Kaatz, M.; Sturm, A.; Elsner, P.; König, K.; Bückle, R.; Köhler, M.J. Depth-resolved measurement of the dermal matrix composition by multiphoton laser tomography. *Skin Res Tech* **2010,** *16,* 131-136 / DOI 10.1111/j.1600-0846.2009.00423.x
42. Lutz, V.; Rahn, C.D.; Puschmann, S. Determination of skin aging in vivo using multi photon laser scanning microscopy (mplsm) in the stratum granulosum. *Journal of investigative Dermatology* **2010,** *130,* S22-S22.
43. Köhler, M.J.; Preller, A.; Elsner, P.; König, K.; Hipler, U.C.; Kaatz, M. Non-invasive evaluation of dermal elastosis by in vivo multiphoton tomography with autofluorescence lifetime measurements. *Exp Dermatol* **2012,** *21(1),* 48-51. DOI: 10.1111/j.1600-0625.2011.01405.x.
44. Puschmann, S.; Rahn, C.D.; Wenck, H.; Gallinat, S.; Fischer, F.F. Approach to quantify human dermal skin aging using multiphoton laser scanning microscopy. *Journal of Biomedical Optics* **2012,** *17,* 036005. DOI: 10.1117/1.JBO.17.3.036005.
45. Lutz, V.; Sattler, M.; Gallinat, S.; Wenck, H.; Poertner, R.; Fischer F. Impact of collagen crosslinking on the second harmonic generation signal and the fluorescence lifetime of collagen autofluorescence. *Skin Research and Technology* **2012,** *18 (2),* 168-179.
46. Lutz, V.; Sattler, M.; Gallinat, S.; Wenck, H.; Poertner, R.; Fischer F. Characterization of fibrillar collagen types using multi-dimensional multiphoton laser scanning microscopy. *International journal of cosmetic science* **2012,** *34 (2),* 209-215.
47. Puschmann, S.; Rahn, C.D.; Wenck, H.; Gallinat, S.; Fischer, F. In vivo quantification of human dermal skin aging using SHG and autofluorescence. *Multimodal Biomedical Imaging* **2012,** *VII 8216,* 41-54.
48. Seidenari, S.; Schianchi, S.; Azzoni, P.; Benassi, L.; Borsari, S.; Cautela, J.; Ferrari, C.; French, P.; Giudice, S.; König, K.; Magnoni, C.; Talbot, C.; Dunsby, C. High-resolution multiphoton tomography and fluorescence lifetime imaging of UVB-induced cellular damage on cultured fibroblasts producing fibres. *Skin Res Tech* **2013,** *19,* 251–257. DOI: 10.1111/srt.12034.
49. Pittet, J.C.; Freis, O.; Vazquez-Duchêne, M.D.; Périé, G.; & Pauly, G. Evaluation of elastin/collagen content in human dermis in-vivo by multiphoton tomography - Variation with depth and correlation with aging. *Cosmetics* **2014,** *1(3),* 211–221. DOI: 10.3390/cosmetics1030211.
50. Pena, A.M.; Baldeweck, T.; Decencière, E.; Koudoro, S.; Victorin, S.; Raynaud, E.; Ngo, B.; Bastien, P.; Brizion, S.; Tancrède-Bohin, E. In vivo multiphoton multiparametric 3D quantification of human skin aging on forearm and face. *Scientific reports* **2022,** *12. DOI: 10.1038/s41598-022-18657-z.*
51. Schindele, A.; Breunig, H.G.; König, K. Multiphoton Tomography for in vivo skin age determination. *Optik & Photonik* **2018,** *2,* 56-59. DOI: 10.22028/D291-29625.

52. Sugata, K.; Osanai, O.; Sano, T.; Takema, Y. Evaluation of photoaging in facial skin by multiphoton laser scanning microscopy. *Skin Res Tech* **2011,** *17(1),* 1–3. DOI: 10.1111.j.1600-0846.2010.00475.x.
53. Miyamoto, K.; Kudoh, H. Quantification and visualization of cellular NAD(P)H in young and aged female facial skin with in vivo two-photon tomography. *British Journal of Dermatology* **2023,** *169,* 25-31. DOI: 10.1111/bjd.12370.
54. Liu, D.C.; Raphael, A.P.; Sundh, D.; Grice, J.E.; Soyer, H.P.; Roberts, M.S.; Prow, T.W. The Human Stratum Corneum Prevents Small Gold Nanoparticle Penetration and Their Potential Toxic Metabolic Consequences. *Journal of Nanomaterials* **2012.**
55. Darvin, M.E.; König, K.; Kellner-Höfer, M.; Breunig, H.G.; Werncke, W.; Meinke, M.C.; Patzelt, A.; Sterry, W.; Lademann, J. Safety assessment by multiphoton fluorescence/second harmonic generation/hyper-Rayleigh scattering tomography of ZnO nanoparticles used in cosmetic products. *Skin Pharmacol Physiol* **2012,** *25,* 219–226. DOI: 10.1159/000338976.
56. Breunig, H.G.; Weinigel, M.; König, K. In vivo imaging of ZnO Nanoparticles from sunscreen on human skin with a mobile multiphoton tomograph. *BioNanoScience* **2014,** *5,* 42-47. DOI: 10.1007/s12668-014-0155-4.
57. Holmes, A.; Thorling, C.; Liu, X.; Liang, X.; Wang, H.; Breunig, H.G.; König, K.; Studier, H.; Roberts, M.S. Revealing interaction of dyes and nanomaterials by multiphoton imaging. In: König, K.; (ed.) *Multiphoton Tomography and Fluorescence Lifetime Imaging* (De Gruyter) **2018,** 346-368. DOI: 10.1515_9783110429985-020.
58. Luengo, J.; Weiss, B.; Schneider, M.; Ehlers, A.; Stracke, F.; König, K.; Kostka, K.H.; Lehr, C.M.; Schäfer. U.F. Influence of nanoencapsulation on human skin transport of flufenamic acid. *Skin Pharmacol Physiol.* **2006,** *19(4),* 190-197. DOI: 10.1159/000093114.
59. Roberts, M.S.; Dancik, Y.; Prow, T.W.; Thorling, C.A.; Lin, L.L.; Grice, J.E.; Robertson, T.A.; König, K.; Becker, W. Non-invasive imaging of skin physiology and percutaneous penetration using fluorescence spectral and lifetime imaging with multiphoton and confocal microscopy. *European Journal of Pharmaceutics and Biopharmaceutics* **2011,** *77,* 469-488 / DOI: 10.1016/j.ejpb.2010.12.023.
60. König, K. Multiphoton Tomography of Intratissue Tattoo Nanoparticles. SPIE-Procced. **2013,** *8207,* 82070S. DOI: 10.1117/12.908128.
61. Nguyen, L.; Mess, C.; Schneider, S.W.; Huck, V.; Herberger, K. In vivo visualisation of tattoo particles using multiphoton tomography and fluorescence lifetime imaging. Exp Dermatol **2022,** *31(11),* 1712-1719.
62. Kröger, M.; Schleusener, J.; Lademann, J.; Meinke, M.C.; Jung, S.; Darvin, M.E. Tattoo pigments are localized intracellularly in the epidermis and dermis of fresh and old tattoos – in vivo study using two-photon excited FLIM. *Dermatology* 2023, 2. DOI: 10.1159/000529577.
63. Anilkumar, V.; König, A., König, K. Imaging Microplastics with Multiphoton Tomographs. Proceed. SPIE 2024, 1284719.
64. König, K.; Ehlers, A.; Stracke, F.; Riemann, I. In vivo drug screening in human skin using femtosecond laser multiphoton microscopy. *Skin Pharmacol Physiol* **2006,** *19(2),* 78-88. DOI: 10.1159/0000919741.
65. Stracke, F.; Weiss, B.; Lehr, C.M.; König, K.; Schäfer, U.F.; Schneider, M. Multiphoton microscopy for the investigation of dermal penetration of nanoparticle-borne drugs. *J Invest Dermatol* **2006,** *126,* 2224-2233. DOI: 10.1038/sj.jid.5700374
66. Madani, H.A.E.; Tancrède-Bohin, E.; Bensussan, A.; Colonna, A.; Dupuy, A.; Bagot, M.; Pena, A.M. In vivo multiphoton imaging of human skin: Assessment of topical corticosteroid-induced epidermis atrophy and depigmentation. *Journal of Biomedical Optics* **2012.** Doi: 10.1117/1.JBO.17.2.026009.
67. Alex, A.; Frey, S.; Angelene, H.; Neitzel, c.D.; Li, J.; Bower, A.J.; Spillman, D.R.; Marjanovic, M.; Chaney, E.J.; Medler, J.L.; Lee, W.; Vasist Johnson, L.S.; Boppart, S.A.; Arp, Z. In situ bio-distribution and residency of a topical anti-inflammatory using fluorescence lifetime imaging microscopy. *British Journal of Dermatology* **2018,** *179.* DOI:10.1111/bjd.16992
68. Tancrède-Bohin, E.; Baldeweck, T.; Brizion, S.; Decencière, E.; Victorin, S.; Ngo, B.; Raynaud, E.; Souverain, L.; Baot, M.; Pena, A.M. In vivo multiphoton imaging for non-invasive time course assessment of retinoids effects on human skin. *Skin Res Tech* **2020,** *26(6),* 794–803. DOI: 10.1111/srt.12877.
69. Bhardwaj, V.; Andler, M.Z.; Mao, J.; Azadegan, C.; Panda, P.K.; Breunig, H.G.; Wenskus, I.; Diaz, I.; König, K. A novel professional-use synergistic peel technology to reduce visible hyperpigmentation on face:

Clinical evidence and mechanistic understanding by computational biology and optical biopsy. *Exp Dermatol* **2024,** *33,* e15069. DOI: 10.1111/exd.15069.

70. Nguyen L et al. Intravital monitoring of psoriasis treatment response and drug delivery using multiphoton fluorescence lifetime imaging. *Exp Dermatol.* in press.
71. Manstein, D.; Herron, G.S.; Sink, R.K.; Tanner, H.; Anderson, R.R. Fractional photothermolysis: a new concept for cutaneous remodeling using microscopic patterns ot thermal injury. *Lasers Surg Med* **2004,** *34,* 426-438. DOI: 10.1002/lsm.20048.
72. Anderson, R.; Parish, J.A. Selective thermolysis: precise microsurgery by selective absorption of pulsed radiation. Science **1983,** *220,* 524-527.
73. Haykal D., Cartier H., Maire C., Mordon S. Picosecond laser in cosmetic dermatology: where are we now? An overview over types and indications. Lasers in Medical Science **2024,** *39,* 8. DOI: 10.1007/s10103-023-03945-5.
74. Balu, M.; Lentsch, G.; Korta, D.Z.; König, K.; Kelly, K.M.; Tromberg, B.J.; Zachary, C.B. In vivo multiphoton microscopy of picosecond -laser induced optical breakdown in human skin. *Lasers Surg Med* **2017,** *49,* 555-562. DOI: 10.1002/lsm.22655
75. Serna, A.; Marcotegui, B.; Decencière, E.; Baldeweck, T.; Pena, A.M.; Brizion, S. Segmentation of elongated objects using attribute profiles and area stability: Application to melanocyte segmentation in engineered skin. *Pattern Recognition Letters* **2014,** *47,* 172-182. DOI: 10.1016/j.patrec.2014.03.014.
76. Bai, B.; Yang, X.; Li, Y.; Zhang, Y.; Pillar, N.; Ozcan, A. Deep learning-enabled virtual histological staining of biological samples. *Light: Science and Applications* **2023,** *57,* doi.org/10.1038/s41377-023-01104-7
77. Decencière, E.; Tancrède-Bohin, E.; Dokladal, P.; Koudoro, S.; Pena, A.M.; Baldeweck, T. Automatic 3D segmentation of multiphoton images: A key step for the quantification of human skin**.** *Skin Res Tech* **2013.** DOI: 10.1111/srt.12019.
78. Guimaraes, P.; Batista, A.; Zieger, M.; Kaatz, M.; König, K. Artificial Intelligence in Multiphoton Tomography: Atopic Dermatitis Diagnosis. *Scientific Reports* **2020,** *10,* 7968. DOI: 10.1038/s41598-020-64937-x.
79. Prinke, P.; Haueisen, J.; Klee, S.; Rizqie, M.; Supriyanti, E.; König, K.; Breunig, H.G.; Piatek, L.; Automatic segmentation of skin cells in multiphoton data using multi-stage merging. *Sci. Rep.* **2021,** *11,* 14534. DOI: 10.1038/s41598-021-93682-y.
80. Lange, I.; Prinke, P.; Klee, S.; Piatek, L.; Warzecha, M.; König, K.; Haueisen, J. Feature-based Differentiation of Malignant Melanomas, Lesions, and Healthy Skin in Multiphoton Tomography Skin Images. *Current Directions in Biomedical Engineering*. **2022,** *8,* 45-48. DOI: 10.1515/cdbme-2022-1013.
81. Li, H.; Pan, Y.; Zhao, J.; Zhang, L. Skin disease diagnosis with deep learning. A review. *Neurocomputing* **2021,** *464,* 364-393. DOI: 10.1016/.neucom.2021.08.096.
82. Benati, E.; Bellini, V.; Borsari, S.; Dunsby, C.; Ferrari, C.; French, P.; Guanti, M.; Guardioli, D.; König, K.; Pellacani, G.; Ponti, G.; Scianchi, S.; Talbot, C.; Seidenari, S. Quantitative evaluation of healthy epidermis by means of multiphoton microscopy and fluorescence lifetime imaging microscopy. *Skin Res Tech* **2011**, 17(3), 295-303. DOI: 10.1111/j.1600-0846.2011.00496.x.
83. König, K. Medical femtosecond laser. *Journal of the European Optical Society-Rapid Publications* **2032,** 19(2), 36. DOI: 10.1051/jeos/2023032.
84. König, K. Multiphoton tomography (MPT). In K. König (Ed.), *Multiphoton microscopy and fluorescence lifetime imaging: Applications in biology and medicine*, Germany: De Gruyter 2018, pp. 247–268. DOI: 10.1515_9783110429985-020.
85. Fast, A.; Lal, A.; Durkin, A.F.; Lentsch, G.; Harris, R.M.; Zachary, C.B.; Ganesan, A.K.; Balu, M. Fast, large area multiphoton exoscope (FLAME) for macroscopic imaging with microscopic resolution of human skin. *Scientific Reports* **2020,** *10,* 18093. DOI: 10.1038/s41598-020-75172-9.